Expanded View Figures

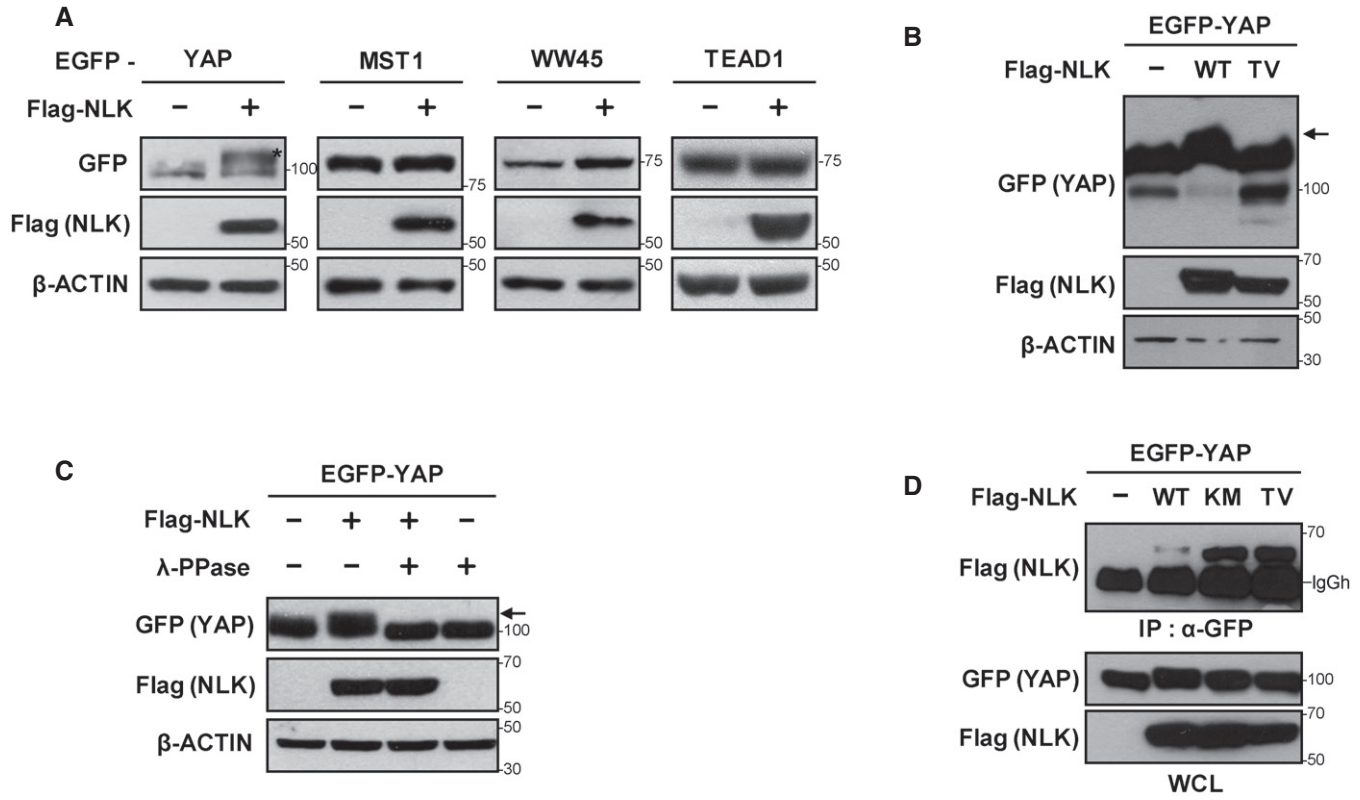

Figure EV1. NLK induces mobility shift of YAP.

A NLK induces mobility shift of YAP but not other Hippo signaling components. HEK293T cells were transfected with plasmids indicated in the figure, and cell lysates were analyzed by immunoblotting (IB) with antibodies shown on the left.

B Mobility shift of EGFP-YAP by NLK in Phos-tag-PAGE gel. Cell lysates from HEK293T cells transfected with indicated plasmids shown in the figure were separated in Phos-tag-PAGE gel, followed by immunoblotting with indicated antibodies. Arrows indicates phosphorylated form of GFP-YAP.

C Removal of mobility shift by treatment with λ-phosphatase. Mobility shift of EGFP-YAP by co-expression of Flag-NLK was eliminated by treatment with λ-phosphatase. Cell lysates were incubated with or without λ-phosphatase and separated by SDS–PAGE, followed by immunoblotting with the indicated antibodies. Arrow indicates phosphorylated form of GFP-YAP.

D NLK interacted with YAP. EGFP-YAP was transfected with empty vector (−), Flag-NLK-WT, Flag-NLK-KM, or Flag-NLK-TV (T286V) into HEK293T cells. EGFP-YAP was immunoprecipitated with anti-GFP antibody, followed by immunoblotting with anti-Flag antibody.

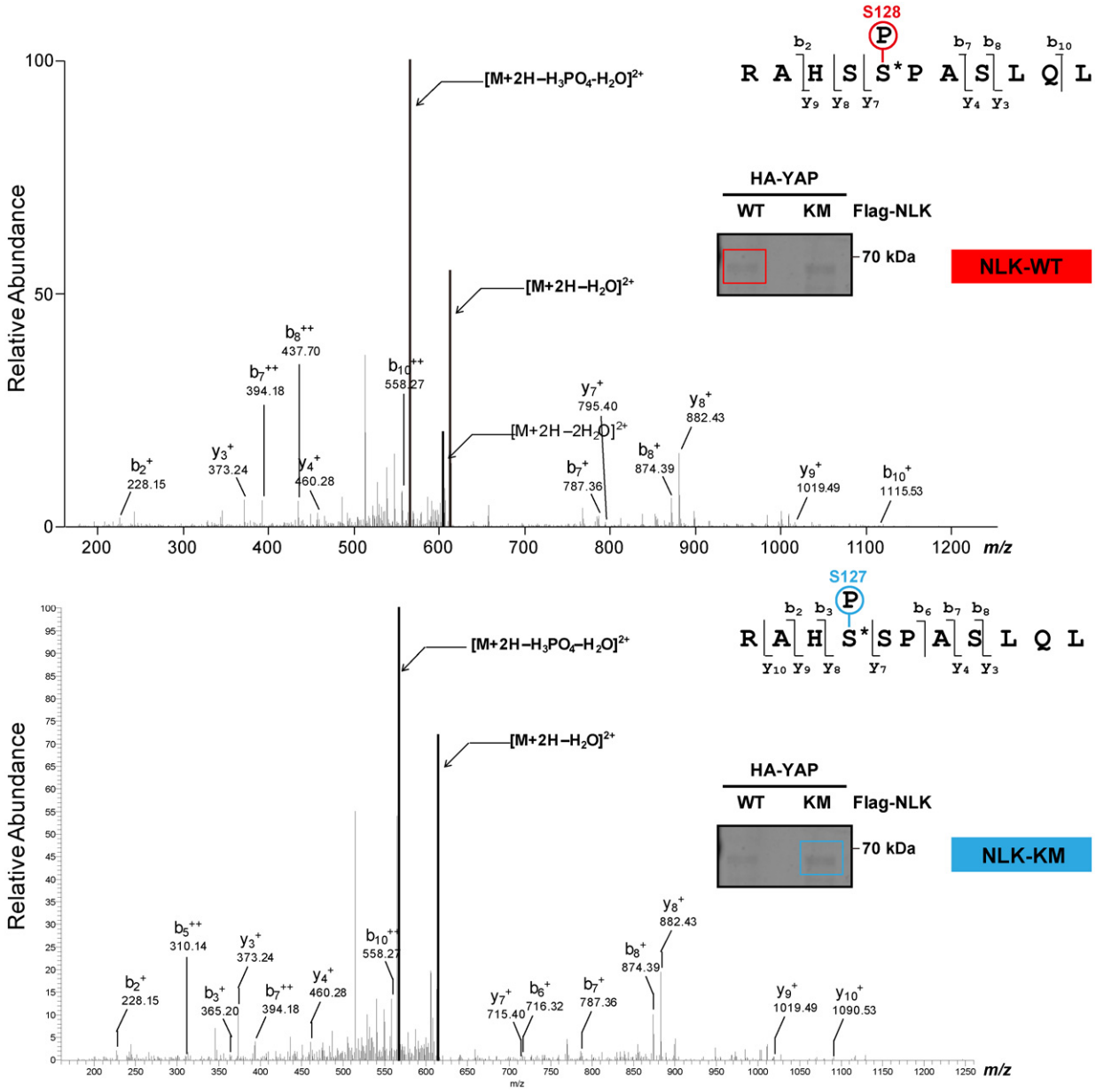

Figure EV2. Ser128 of YAP is a target residue of NLK.

LC-MS/MS analysis revealed phospho-peaks of YAP-S128 by the expression of NLK-WT (upper panel) and phospho-peaks of YAP-S127 by NLK-KM (lower panel). HA-YAP was transiently transfected into HEK293T cells along with either Flag-NLK-WT or Flag-NLK-KM, and then, HA-YAP was immunoprecipitated with anti-HA antibody. Immunoprecipitates were separated on SDS–PAGE and stained with Coomassie blue. HA-YAP bands were cut out, and LC-MS/MS analysis was performed. Figures show the LC-MS/MS spectra for the phosphorylation of Ser128(RAHSS*PASLQL) or Ser127(RAHS*SPASLQL), respectively (indicated by asterisks). Red and blue boxes indicate cutting areas for LC-MS/MS analysis.

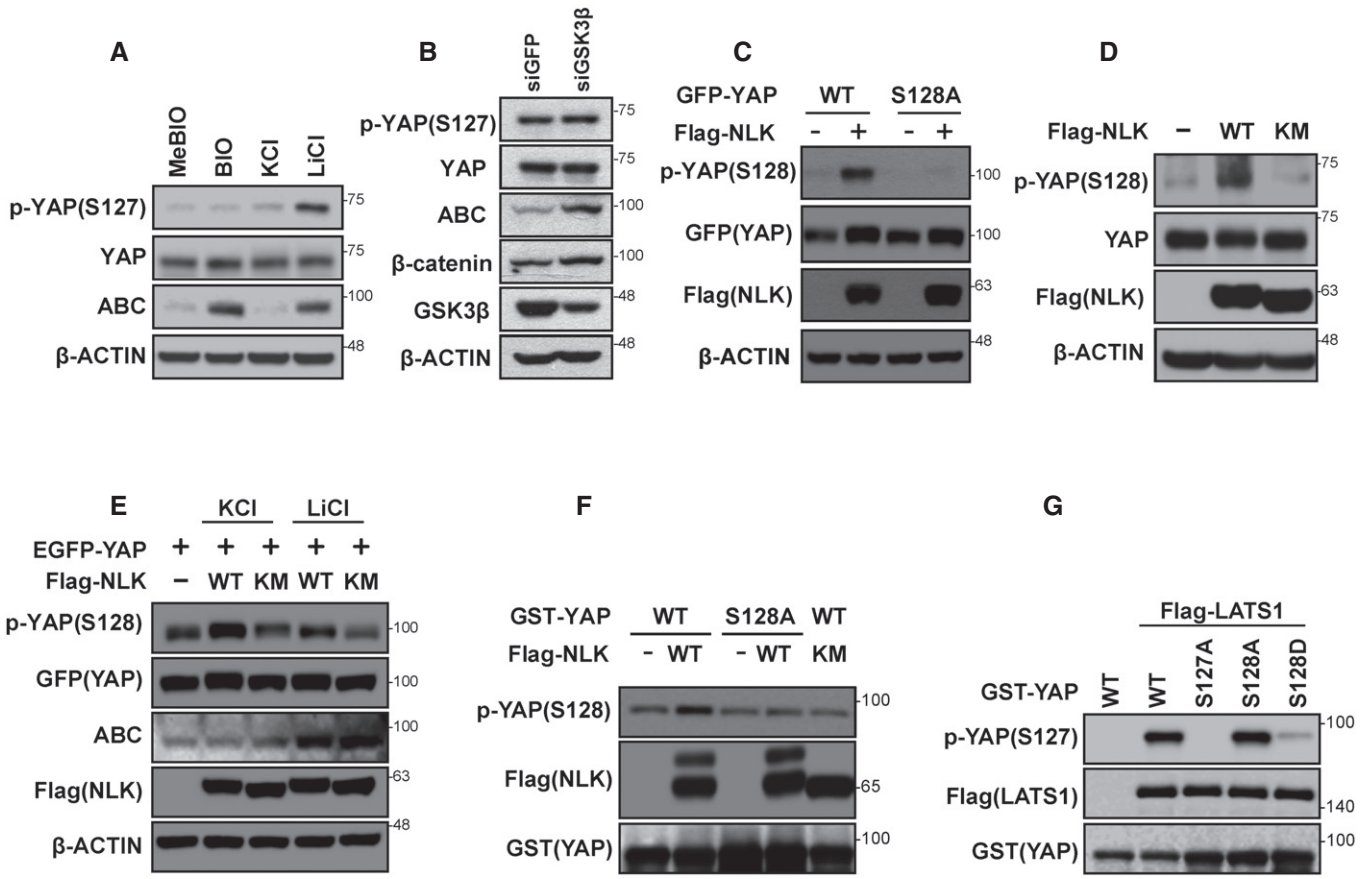

Figure EV3. Phosphorylations of Ser127 and Ser128 of YAP may be mutually exclusive.

A Inhibition of NLK induces phosphorylation at Ser127 of YAP. HEK293T cells were treated with either 6-bromoindirubin-3′-oxime (BIO, 4 μM; inhibitor of GSK3β), or lithium chloride (50 mM; inhibitor of GSK3β and NLK). MeBIO (4 μM) or KCl (50 mM) were used as negative controls for BIO or LiCl, respectively.

B Knockdown of GSK3β has no effect on YAP phosphorylation at Ser127. Lysates from HEK293T cells transfected with either siControl or siGSK3β were immunoblotted with antibodies indicated in the figure.

C YAP phosphorylation at Ser128 by NLK. Cell lysates from HEK293 cells transfected with empty vector (—), EGFP-YAP, EGFP-YAP-S128A, and Flag-NLK-WT were immunoblotted with antibodies shown in the figure.

D Ectopic expression of wild-type NLK, but not kinase-negative NLK, enhanced the level of endogenous phospho-YAP(Ser128). Cell lysates from HEK293T cells transfected with empty vector (—), Flag-NLK-WT, or Flag-NLK-KM were immunoblotted with antibodies indicated in the figure.

E Treatment with LiCl attenuated NLK-mediated phosphorylation of YAP Ser128. Cell lysates from HEK293 cells transfected with empty vector (—), Flag-NLK-WT, or Flag-NLK-KM and treated KCl or LiCl. Lysates were immunoblotted with antibodies shown in the figure.

F NLK specifically phosphorylates YAP-S128 *in vitro*. GST-YAP or GST-YAP(S128A) was incubated with immunoprecipitated Flag-NLK-WT or Flag-NLK-KM from lysates of HEK293T cells transfected with Flag-NLK-WT or Flag-NLK-KM as indicated in the figure. The level of phosphorylation at S128 was detected with pYAP-S128 antibody.

G Phosphorylation of S128 by NLK inhibits phosphorylation of YAP-S127 by LATS1. Immunoprecipitated Flag-LATS1 from lysates of HEK293T cells transfected with Flag-LATS1 was incubated with various mutant forms of GST-YAP as shown in the figure. The level of phosphorylation at S127 was detected with pYAP-S127 antibody.

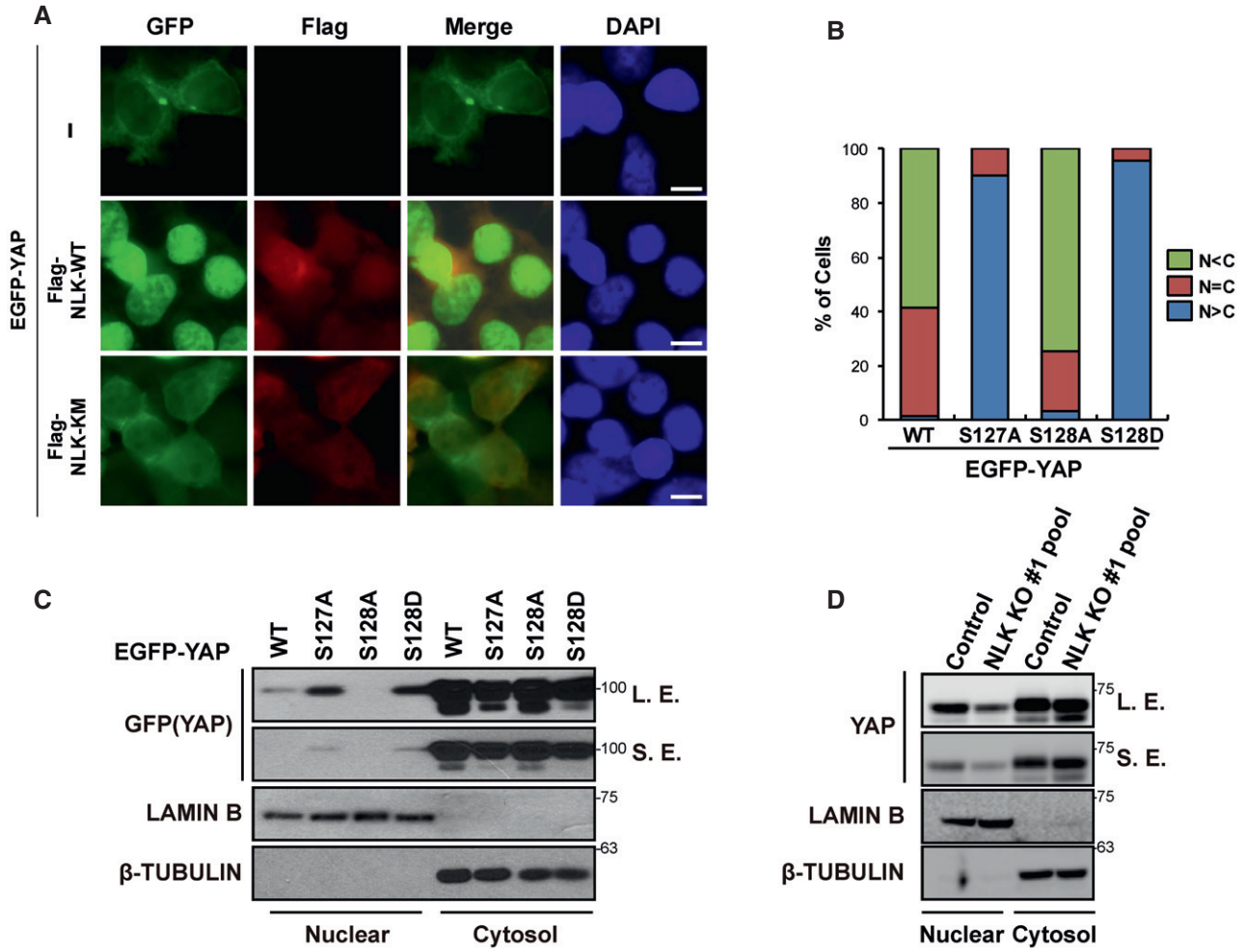

Figure EV4. NLK-mediated phosphorylation at Ser128 leads to nuclear localization of YAP.

A Overexpression of NLK-WT, but not NLK-KM, induces nuclear localization of EGFP-YAP. Immunofluorescence analysis was performed in HEK293T cells transfected with EGFP-YAP along with empty vector (–), Flag-NLK-WT, or Flag-NLK-KM. Scale bars: 10 μm.

B Summary of subcellular localization of EGFP-YAP, EGFP-YAP-S127A, EGFP-YAP-S128A, or EGFP-YAP-S128D, as shown in Fig 3D.

C Phosphorylation status of Ser127 or Ser128 determines subcellular localization of YAP. Nuclear and cytosolic fractions of lysates were prepared and immunoblotted with antibodies indicated in the figure. Lamin B and β-tubulin were used as markers for nuclear and cytosolic fractions, respectively. S.E., short exposure; L.E., long exposure.

D Depletion of NLK leads to reduction in YAP levels in the nuclear fraction. Lysates from NLK knockout HEK293 cells were immunoblotted with antibodies indicated in the figure. Lamin B and β-tubulin were used as markers for nuclear and cytosolic fractions, respectively. S.E., short exposure; L.E., long exposure.

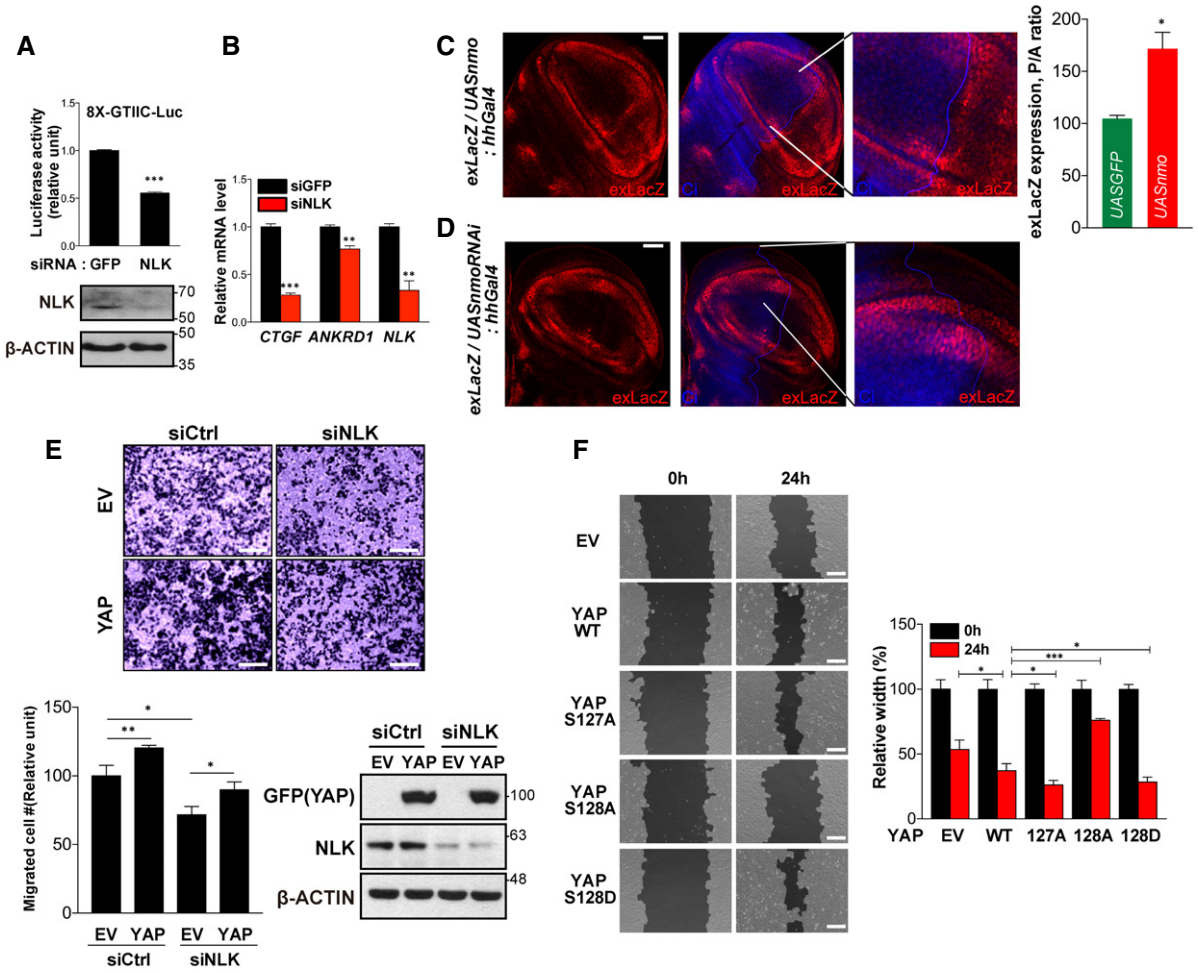

Figure EV5. NLK positively regulates YAP activity in physiological settings.

A Knockdown of NLK attenuates YAP-dependent reporter activity. HEK293T cells were transfected with siRNA for GFP or NLK, and *8xGTIIC* promoter-driven luciferase activity was measured. Luciferase activities represent average values from a representative of multiple experiments performed in triplicate. Error bars indicate standard deviations of triplicate measurements. Lysates were immunoblotted with indicated antibodies. ***$P < 0.005$. Student's *t*-test was used for statistical analysis.

B Knockdown of NLK reduces endogenous YAP/TEAD target gene expression. Quantitative real-time PCR analyses were performed with RNAs from HEK293T cells transfected with siRNA for GFP or NLK. The expression of *ANKRD1*, *CTGF*, and *NLK* mRNA was normalized with the level of *β-actin*. Data represent average values from a representative of multiple experiments performed in triplicate. Error bars indicate standard deviations of triplicate measurements. Data are presented as mean ± SD. **$P < 0.01$ and ***$P < 0.005$. Student's *t*-test was used for statistical analysis.

C Overexpression of *nemo* achieved in the posterior compartment of wing imaginal discs (marked by the absence of anti-Ci staining, blue) using the *hh-Gal4* driver results in expression of the *yki* target gene expanded (exLacZ, red) within the wing pouch, where it is normally expressed only at low levels. The third panel shows a higher magnification of a relevant area. The unaffected anterior domain serves as an internal control (left panel). Quantification of exLacZ levels achieved upon posterior overexpression of *nemo*, measured as normalized posterior-to-anterior levels and compared to similar expression of GFP (right panel). Data are presented as mean ± SEM, $n = 5$ discs. *$P < 0.05$. Student's *t*-test was used for statistical analysis. Scale bar: 50 μm.

D Downregulation of *nemo* with RNAi achieved in the posterior compartment of wing imaginal discs (marked by the absence of Ci) results in decreased expression of the *exLacZ* in the periphery of the wing pouch, where it is normally expressed at high levels. The third panel shows a higher magnification of a relevant area. Two different RNAi constructs produce identical effect. Scale bar: 50 μm.

E Ectopic expression of YAP rescues retarded cell migration ability induced by knockdown of NLK. HeLa cells were transfected with control or NLK-targeting siRNA and empty vector (EV) or EGFP-YAP as shown in the figure. Migratory cells on lower face membrane were stained by crystal violet (upper panel). Scale bars: 200 μm. Graphs show relative migrated cell number from a representative of multiple experiments performed in triplicate (left bottom panel). Error bars indicate standard deviations of triplicate measurements. Data are presented as mean ± SD. *$P < 0.05$ and **$P < 0.01$. Student's *t*-test was used for statistical analysis. Lysates from the cells transfected as above were immunoblotted as shown on the bottom right panel.

F Mutant forms of YAP which have different phosphorylation status of Ser127 or S128 differentially regulate wound healing ability. HEK293 cells were transfected with indicated plasmids in the figure, and the wounded areas after 0 and 24 h were measured by using the TScratch program (left panel). EV, empty vector. Graphs show relative values of unfilled areas and average values from a representative of multiple experiments performed in triplicate (right panel). Error bars indicate standard deviations of triplicate measurements. Data are presented as mean ± SD. *$P < 0.01$ and ***$P < 0.005$. Student's *t*-test was used for statistical analysis. Scale bars: 200 μm.